Associative networks of cholesterol-modified dextran with short and long micelles

Hala Afifi, Marcelo Alves da Silva, Cécile Nouvel, Jean-Luc Six, Christian Ligoure, Cécile A. Dreiss

1

Associative networks of cholesterol-modified dextran with short and long micelles

Hala Afifi, Marcelo A. da Silva, Cécile Nouvel, Jean-Luc Six, Christian Ligoure and Cécile A. Dreiss*

Short (rod-like) and long (wormlike) micelles based on the surfactant polyoxyethylene cholesteryl ether associate with cholesterol-modified dextran to form solid-like networks.

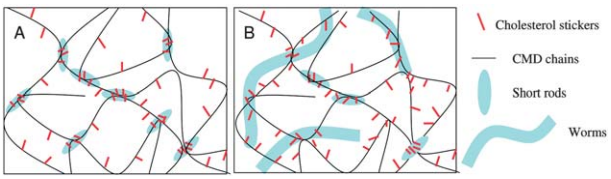

Please check this proof carefully. **Our staff will not read it in detail after you have returned it**.

Translation errors between word-processor files and typesetting systems can occur so the whole proof needs to be read. Please pay particular attention to: tabulated material; equations; numerical data; figures and graphics; and references. If you have not already indicated the corresponding author(s) please mark their name(s) with an asterisk. Please e-mail a list of corrections or the PDF with electronic notes attached – do not change the text within the PDF file or send a revised manuscript.

Please bear in mind that minor layout improvements, e.g. in line breaking, table widths and graphic placement, are routinely applied to the final version.

We will publish articles on the web as soon as possible after receiving your corrections; no late corrections will be made.

Please return your **final** corrections, where possible within **48 hours** of receipt by e-mail to: softmatter@rsc.org

Reprints—Electronic (PDF) reprints will be provided free of charge to the corresponding author. Enquiries about purchasing paper reprints should be addressed via: http://www.rsc.org/publishing/journals/guidelines/paperreprints/. Costs for reprints are below:

Reprint costs

No of pages	Cost (per 50 copies)	
	First	Each additional
2–4	£225	£125
5–8	£350	£240
9–20	£675	£550
21–40	£1250	£975
>40	£1850	£1550

Cost for including cover of journal issue:
£55 per 50 copies

Associative networks of cholesterol-modified dextran with short and long micelles

Hala Afifi,[a] Marcelo A. da Silva,[a] Cécile Nouvel,[b] Jean-Luc Six,[b] Christian Ligoure[cd] and Cécile A. Dreiss*[a]

Received 10th March 2011, Accepted 7th February 2011
DOI: 10.1039/c1sm05416c

The strong associative behaviours between cholesterol-modified dextran (CMD) and short and long polyoxyethylene cholesteryl ether ($ChEO_{10}$) micelles were investigated using rheology and small-angle neutron scattering (SANS). In solutions of short rod-like micelles ($ChEO_{10}$ alone), the addition of 5.0 wt% CMD induced a remarkable transition from a Newtonian system to a highly solid-like viscoelastic network, with an increase in zero-shear viscosity of over 5 orders of magnitude. The frequency sweeps at $ChEO_{10}$ concentrations above 2.5 wt% were fitted to a Maxwell model with 3 elements and, quite remarkably, fell onto a single master curve, while no network was formed at 2.5 wt% micelles. Viscoelastic solutions of wormlike micelles (WLMs) were obtained by adding the co-surfactant triethylene glycol monododecyl ether ($C_{12}EO_3$) to $ChEO_{10}$ solutions at a constant $ChEO_{10}/C_{12}EO_3$ ratio of 5/1. The introduction of CMD into the WLM solutions induced a transition to a more liquid-like behaviour (G''/G' increased), however both moduli increased by one order of magnitude. At the lowest $ChEO_{10}$ concentration (2.5%), the solid-like behaviour was lost. Overall, a comparable rheological response was obtained for the WLM and the short rods with CMD, however the WLM/CMD behaviour suggested a wider spectrum of relaxation processes, longer relaxation times and higher plateau moduli. SANS data from the polymer/micelles mixtures displayed a strong structural peak and were remarkably identical for both $ChEO_{10}$/CMD and $ChEO_{10}/C_{12}EO_3$/CMD systems, suggesting a very similar type of network structure, independently of the initial size of the micelles. Overall, all the results taken together show a very high affinity between the polymer and the micelles and suggest a breakup of the WLM induced by CMD. The resulting network is constituted by polymeric chains connected by micellar aggregates through hydrophobic interactions between the micellar cholesterol cores and the pendent cholesterol moieties of the polymer.

Introduction

Wormlike micelles (WLMs) are very long, semi-flexible surfactant aggregates, which, above a system-dependent concentration, known as the overlap concentration, entangle into a transient network, imparting remarkable viscoelastic properties to their solutions.[1–3] Their behaviour is analogous to the one observed in polymer solutions, however unlike polymers wormlike micelles constantly break and reform, providing additional relaxation mechanisms. One obvious advantage over polymers therefore is that they are stable under high shear rates and can recover their supramolecular structure. They have therefore been referred to as 'living polymers'.[4,5] The rich rheological response of WLM has led to their exploitation in various industrial processes such as fracturing fluids in oil fields, cooling fluids, liquid dish-washing detergents and personal care products such as shampoos and body soaps.[6–12]

Similarly, a rich rheological behaviour has been observed in solutions of associative polymers or hydrophobically modified polymers (HMPs), which are water-soluble polymers with hydrophobic pendant groups[13–21] (often referred to as 'stickers'). Interest in HMP primarily started for applications in oil recovery and rheological control of paints and coatings[22–25] but their interest now extends to the biomedical field.[26–28]

In view of the above, the combination of HMP and wormlike micelles seems to be an attractive option. In fact, it has been shown that combining WLM and hydrophobically modified polymers can lead to significantly enhanced viscoelastic properties compared to the individual components at the same concentration.[29,30] This has obvious environmental and cost consequences as rheological control can be achieved with less material. Surfactant/polymer interactions have been studied intensively in the past decades and are used in numerous technological applications,[31–36] but most of these studies have dealt

[a]*King's College London, Institute of Pharmaceutical Science, 150 Stamford Street, SE1 9NH, UK*
[b]*Laboratoire de Chimie Physique Macromoléculaire, UMR 7568 CNRS-Nancy University, ENSIC, BP 20451, 54001 Nancy Cedex, France*
[c]*Université Montpellier 2, Laboratoire Charles Coulomb UMR 5221, F-34095 Montpellier, France*
[d]*CNRS, Laboratoire Charles Coulomb UMR 5221, F-34095, Montpellier, France*

with low concentrations of surfactant or spherical micelles, while a much more limited number of reports can be found on polymer/wormlike micelle interactions.[14,29,30,34,37–43]

Polymers can either destroy or strengthen the transient networks formed by wormlike micelles. Polyethylene glycol and poly(propylene glycol) for instance were reported to induce the disruption of the micellar network in aqueous solutions of potassium oleate[34] and cetyltrimethylammonium salicylate,[44] due to the transition from cylindrical to spherical micelles. This behaviour was attributed to the wrapping-up of the hydrophobic polymer chains around the surface of the surfactant micelles. As the surface/volume ratio is larger for spherical micelles than for cylindrical, rod-to-sphere transition takes place, optimising the shielding of the polymer from water. In other scenarios, oppositely charged polymer added to the anionic surfactant potassium oleate favoured micellar growth instead,[37] while the hydrophobic polymer poly(propyleneglycol) led to a drastic reduction in the viscoelastic properties of cetyltrimethylammonium bromide wormlike micelles without notable structural change.[40]

With hydrophobically modified polymers (HMPs), where the hydrophobic moieties are distributed along the polymeric chains, different effects on the wormlike micelle structures have been reported, which are reflected by changes in the rheological properties.[41] For instance, HMP can cross-link WLM by intercalation of the stickers into the WLM cores, forming a network where some relaxation modes are linked to sticker pullout time.[41,45] The opposite behaviour—surfactants cross-linking the polymer—has also been observed.[14] In this case, the WLMs break down and reform as shorter (spherical or cylindrical micelles) in order to better shield the stickers from the solvent.

In this contribution, we report a considerable enhancement of the rheological response in a system based on biocompatible and biodegradable components, namely, the association between cholesterol-modified dextran (CMD) and the surfactant polyoxyethylene cholesteryl ether ($ChEO_{10}$). We investigate and compare two types of networks formed in the presence of the modified dextran: one formed with short (rod-like) micelles and one formed with long entangled wormlike micelles.

Polyoxyethylene cholesterol surfactants ($ChEO_n$) are unique nonionic surfactants which are characterised by a strong segregation between their hydrophilic headgroups and hydrophobic tails compared to conventional alkyl ethoxylated surfactants.[46] Long EO-chain cholesterol surfactants form ellipsoids or short cylindrical micelles.[47,48] However, when they are mixed with short-chain polyoxyethylene alkyl ether-type nonionic surfactants, such as triethylene glycol monododecyl ether ($C_{12}EO_3$) or monoglycerides, they form viscoelastic solutions of long wormlike micelles.[49–51]

Dextran is a biocompatible polymer which was modified in order to optimise the associative interactions with the surfactant's tails, through hydrophobic substitution by cholesterol stickers. By blending CMD and $ChEO_{10}$ micelles, cholesterol–cholesterol interactions between the pendant units of the modified polymer and the hydrophobic cores of the micelles were expected to take place, leading to synergistic effects in the rheological response of the polymer/micellar mixtures.

In the first part of this paper, the rheological behaviour of both the short ($ChEO_{10}$) and long ($ChEO_{10}/C_{12}EO_3$) micelles with CMD is studied and compared using both oscillatory and steady shear experiments. Remarkable changes in the viscoelastic properties of both systems are observed upon addition of CMD, demonstrating a strong association between the polymer and the micelles. In the second part, small-angle neutron scattering measurements are used to bring structural insight into the networks. The combination of the results from both techniques enables us to propose a picture of the organisation of the polymer chains and micelles.

Materials and methods

Materials

Polyoxyethylene cholesteryl ether ($ChEO_{10}$) was purchased from Ikeda Corporation, Yokohama, Japan. Triethylene glycol monododecyl ether ($C_{12}EO_3$) was obtained from Aldrich Chemical Co. Ltd., UK. Dextran T40 ($\bar{M}_n$ = 33 800 g mol^{-1}, polydispersity index (I) = 1.27, as characterised by size exclusion chromatography coupled to multi-angle laser light scattering (SEC-MALLS) in water (0.1 M $NaNO_3$, 6.15 × 10^{-3} M NaN_3)) was purchased from Pharmacia Biotech and dried under reduced pressure at 100 °C overnight. Cholesterol and 1,6-hexyl diisocyanate were purchased from Aldrich and used without any further purification. Toluene (VWR), pyridine (Aldrich) and dimethyl sulfoxide (DMSO, Fischer scientific 99%) were vacuum-distilled before use.

All solutions of surfactants, polymers and their mixtures were made in D_2O (99% purity, Sigma Chemical Co. UK), except those for the cryo-TEM measurements which were prepared in deionised water. All chemicals were used as received unless stated. A glass pycnometer was used to measure the density of $ChEO_{10}$.

Samples preparation

All surfactant solutions were prepared by mixing specific amounts of stock solutions of $ChEO_{10}$ and $C_{12}EO_3$ (20 wt%) in D_2O at room temperature and were vortex-mixed. The polymer-containing samples were prepared using a 10 wt% stock solution of the CMD. All solutions were left to rest at least 48 hours at room temperature and were equilibrated at 25.0 °C (in a water-bath) for 24 hours before conducting the rheological measurements.

Polymer synthesis

The synthetic pathway of the cholesterol-modified dextran (CMD) is a two-step procedure. First, cholesteryl *N*-(6-isocyanatohexyl)carbamate was synthesised using a procedure previously established[52] followed by its condensation with dextran T40. Cholesterol (10 g, 25.8 mmol) was reacted with 1,6-hexyl diisocyanate (62.5 mL, 0.37 mol) in 256 mL of dry toluene in the presence of 5 mL pyridine at 80 °C for 48 hours. The reaction was monitored by thin-layer chromatography (TLC) and after the reaction was completed the solvent was removed *in vacuo*. After adding 600 mL of petroleum ether, the residue was stored overnight at −10 °C. The precipitate obtained was separated and dried *in vacuo* at 30 °C overnight to give a white powder of cholesteryl *N*-(6-isocyanatohexyl)carbamate.

The second step in the synthetic procedure was carried out by adding 0.169 g (0.3 mmol) of cholesteryl *N*-(6-isocyanatohexyl) carbamate to a solution of 4 g dextran (24.8 mmol equiv.) in 100 mL dry dimethyl sulfoxide (DMSO) containing 8 mL pyridine, the reaction mixture was left to stir for 8 hours at 80 °C. The disappearance of cholesteryl *N*-(6-isocyanatohexyl)carbamate was monitored by TLC. Ethanol (500 mL) was added to the reaction mixture and the resulted suspension was left at 4 °C overnight. After filtration, the precipitate was purified by dialysis against ethanol/water (1 : 1) for 48 hours, followed by pure water for another 48 hours. The obtained suspension was then freeze-dried to give a white powder of cholesterol-modified dextran (CMD) with a degree of substitution of 1 cholesterol group per 100 glucose units as determined by ^{1}H NMR in $CDCl_3$.

Rheological measurements

Steady shear and small-amplitude dynamic shear measurements were performed on a dynamic strain-controlled rheometer ARES (TA instruments) using cone-and-plate geometry (25 mm, 0.02 rad), with a Peltier unit for temperature control and a solvent trap to minimise evaporation. Samples were allowed to rest before the start of the experiment to ensure dissipation of any pre-shearing due to loading.

The frequency sweep tests were performed within the linear viscoelastic regime (determined previously by dynamic strain sweep measurements). Measurements were carried out in duplicate or triplicate, with very good reproducibility. The results reported in this work are examples of typical data obtained, not averages. The zero-shear viscosity (η_0) was obtained by extrapolation from the flow curves. Values of the relaxation time τ_r and plateau modulus G_0 were obtained by fitting the frequency sweeps with a multi-element Maxwell model:

$$G'(\omega) = \sum_k G_k \frac{\omega^2 \tau_k^2}{1 + \omega^2 \tau_k^2} \quad (1)$$

$$G''(\omega) = \sum_k G_k \frac{\omega \tau_k}{1 + \omega^2 \tau_k^2} \quad (2)$$

where G' and G'' are the storage and loss moduli, respectively; G_k and τ_k are the G_0 and τ_r for the k^{th} element, respectively; ω is the oscillation frequency and G_0 is defined as:

$$G_0 = \sum_k G_k \quad (3)$$

The fitting was done using the non-linear fitting tool from Microcal Origin™ 6.0 software. Initially, a set of parameters were obtained for the G' curves; this set was then used as initial parameters for fitting G'' and the results were used to generate a new fit for G' data. This process was repeated until a single set of parameters was obtained that provided the best fit for both moduli (which was not necessarily the best fit for each modulus individually). The purpose of the fitting with multiple elements is to provide a more quantitative interpretation of the rheological data. The number of elements chosen was based solely on the minimal number needed to obtain a good fit and they are not attributed a physical meaning. However, they give a useful measure of the departure from the pure Maxwell behaviour.

Samples for rheological measurements were vortex-mixed and kept in a water bath at 25 °C for 24 hours to ensure equilibration before performing the measurements. Samples were made in D_2O to ensure that they were equivalent to the samples used for SANS measurements.

SANS measurements

Small-angle neutron scattering experiments were performed on a LOQ instrument at ISIS pulsed neutron source (ISIS, Rutherford-Appleton Laboratory, STFC, Didcot, Oxford) and on a V4 instrument at the Hahn-Meitner Institute, Berlin, Germany. The LOQ uses incident wavelengths from 2.2 to 10.0 Å, sorted by time-of-flight, with a fixed sample–detector distance of 4.1 m, which provided a range of scattering vectors (q) from 0.009 to 0.29 Å^{-1}. V4 covers a scattering vector (q) range from 0.004 to 0.37 Å^{-1}; the neutrons are collected on a two-dimensional position sensitive detector which was placed at 1, 4 and 12 m horizontally from the sample.

The samples used in the SANS experiments were prepared in D_2O to optimise the contrast with the protonated surfactants and polymer. The samples were placed in clean disc-shaped quartz cells (Hellma) of 1 and 2 mm path length and the measurements were carried out at 25 °C. All scattering data were first normalised for sample transmission and then background-corrected using a quartz cell filled with D_2O (this process also removes the inherent instrumental background arising from vacuum, windows, *etc.*) and finally corrected for the linearity and efficiency of the detector response using instrument-specific software package. The data were then converted to the differential scattering cross-sections (in absolute units of cm^{-1}) using the standard procedures at ISIS[53] and HMI.

SANS data fitting

Data presenting a typical Kratky behaviour in a [$q^2I(q)$ *vs.* q] representation ('bell-shaped' scattering curve with a linear slope at low q) were tested against the Kratky–Porod wormlike chain model, which describes the scattering from elongated objects characterised by their local rigidity.[54,55] In the q range $q > b^{-1}$, where b is the statistical unit length (or persistence length), the scattering cross-section of an infinitely thin wormlike chain is expressed by:

$$\frac{\partial \Sigma}{\partial \Omega}(q) \approx \frac{\pi c (\Delta\rho)^2}{N_A \delta^2} \times \frac{M_L}{q} \quad (4)$$

where $\Delta\rho$ is the contrast, M_L the mass per unit length, equal to (M/n), where n is the number of segments and M the total mass. This expression can be modified by incorporating a Guinier-like factor to take into account a finite cross-section.[54]

$$\frac{\partial \Sigma}{\partial \Omega}(q) \approx \frac{\pi c (\Delta\rho)^2}{N_A \delta^2} \times \frac{M_L}{q} \times \exp\left(-\frac{q^2 R_g^2}{2}\right) \quad (5)$$

where R_g is the cross-sectional radius of gyration, which is related to the cross-sectional radius by $R = \sqrt{2}R_g$. By plotting the data as $\ln\left(q \times \frac{\partial \Sigma}{\partial \Omega}(q)\right)$ *vs.* q^2, a linear plot is obtained with a gradient of $\left(-\frac{R_g^2}{2}\right)$ and an intercept of $\ln\left(\frac{\pi c (\Delta\rho)^2 M_L}{N_A \delta^2}\right)$.

SANS data were also fitted using a model for cylinders. For N randomly oriented rods of length L and radius R the form factor $P(q)$ is given by:

$$P(q) = N \int_0^{\pi/2} F^2(q)\sin(\gamma) d\gamma \quad (6)$$

$$\text{with } F(Q) = (\Delta\rho)V \frac{\sin\left(\frac{1}{2}qL\cos\gamma\right)}{\frac{1}{2}qL\cos\gamma} \frac{2J_1(qR\sin\gamma)}{qR\sin\gamma} \quad (7)$$

where $J_1(x)$ is the first order Bessel function and γ is the angle between the q vector and the axis of the rod.

The data modelling program FISH[56] was used to fit the SANS data. FISH uses standard iterative least-squares fitting in which selected parameters of the chosen model can be refined to optimise the fit. Parameters were refined from several starting points to ensure that a global (rather than a local) minimum was found. A pre-factor, referred to as the 'scale' factor, containing parameters such as volume fraction and contrast was left to float and the value returned by the fit checked against its calculated value to confirm consistency of the fit. A margin of ±20% difference was deemed acceptable. Samples were measured in D_2O to maximise the contrast. Scattering length densities of 4.19 $\times$ 10^{-7} Å^{-2} and 1.33 $\times$ 10^{-8} Å^{-2} were used for $ChEO_{10}$ and $C_{12}EO_3$, respectively. A volume-averaged scattering length density was calculated for the wormlike micelles, using the experimental volume fractions of each surfactant.

Cryogenic Transmission Electron Microscopy

Cryo-TEM measurements were performed with a Zeiss TEM 902A instrument, operating at 80 kV in zero-loss bright-field mode. Digital images were recorded under low dose conditions with a BioVision Pro-SM Slow Scan CCD camera system. An underfocus of 1–2 μm was used in order to enhance the contrast. The preparation procedure has been described in detail elsewhere.[57] Specimens for examination were prepared in a climate chamber with temperature and humidity control (temperature 25 °C and a relative humidity of approximately 98–99%). Thin films of sample solution were prepared by placing a small drop of the sample on a copper grid supported perforated polymer film, covered with thin carbon layers on both sides. After the drop was blotted with filter paper, thin sample films (10–500 nm) spanned the holes in the polymer film. Immediately after blotting, the samples were vitrified by plunging them into liquid ethane, held just above its freezing point. Samples were kept below −165 °C and protected against atmospheric conditions during both transfer to the TEM and examination. Several images were taken of each sample studied, which were all consistent (a representative example is presented here).

Results and discussion

In this work, we compare the effect of cholesterol-modified dextran (CMD) on the associative structures and viscoelastic properties of two types of micelles: short micelles ($ChEO_{10}$) and wormlike micelles (formed by mixtures of $ChEO_{10}$ with $C_{12}EO_3$). The polymer concentration is kept constant at 5.0 wt%. The micellar concentration (based on the amount of ChE_{10}) is varied from 2.5 to 10 wt%, while keeping $ChEO_{10}/C_{12}EO_3$ weight ratio constant at 5 : 1. Upon mixing the different stock solutions, highly viscoelastic solutions form almost instantaneously. In the first part of this study, the linear and non-linear rheological properties of these solutions are discussed. In the second part, the results from SANS measurements on the same systems are analysed, from which a structural arrangement of the micelles/polymer networks is proposed.

Rheological properties

Viscoelastic behaviour. In this study, we compare both the linear and non-linear rheological behaviour of the $ChEO_{10}$/CMD and $ChEO_{10}/C_{12}EO_3$/CMD systems. $ChEO_{10}$ has been found to aggregate in solution as ellipsoids or short rods of *ca.* 170 Å length.[48] Solutions of $ChEO_{10}$ micelles show a Newtonian behaviour with a viscosity of *ca.* 2 mPa s at 25 °C, hence very close to pure water. The polymer solutions display a very weak shear-thinning response with a viscosity only slightly higher than water (data not shown), even at 5.0%. Unlike other HMPs which have been found to self-assemble and lead to a strong viscoelastic response,[58,59] CMD does not form a network on its own. Instead, its solutions are slightly turbid, with the presence of particles visible to the eye, showing limited solubility of the polymer, probably due to aggregation driven by hydrophobic interactions between the cholesterol pendant groups. Note that dextran T40, which was modified to give CMD, is well below the entanglement molecular weight at the concentration studied,[17] which therefore should also be the case for CMD.[17,60] We therefore do not expect to see relaxation processes due to polymer reptation in our systems. The addition of 5.0% CMD to $ChEO_{10}$ or $ChEO_{10}/C_{12}EO_3$ solutions at concentrations above 2.5% induces a remarkable increase in the viscoelastic properties of the micellar solutions and leads to the disappearance of undissolved polymeric particles, as already observed for other HMP/surfactant micelles mixtures.[61] At 2.5% micellar concentration instead, the short $ChEO_{10}$ solutions remain liquid-like, while the $ChEO_{10}/C_{12}EO_3$ wormlike solutions, originally solid-like, become more liquid-like upon addition of the polymer.

Fig. 1 shows the frequency sweep curves for the $ChEO_{10}$/CMD systems studied in this work: 5.0% CMD with 5.0, 7.5 and 10% $ChEO_{10}$. All samples show a characteristic viscoelastic behaviour, reminiscent of the Maxwell model. However, the data do not fit to a single-element Maxwell model and a multi-element model was used instead. The straight lines show the fits obtained for a 3-element Maxwell model (Fig. 1). The values of the parameters obtained are reported in Table 1. There is a very clear, nearly linear increase of the moduli G_{01}, G_{02}, G_{03} and the relaxation times τ_{r1}, τ_{r2}, τ_{r3} with the concentration of $ChEO_{10}$. For simplicity, the rest of the discussion focuses on G_0, the sum of all three moduli obtained from the fits (eqn (3)), and on τ_r, the longest relaxation time, which is substantially higher than the other two, and correlates with the hydrophobic junctions lifetime.[62] This clear trend with concentration is reflected by the construction of a master curve from all three mechanical spectra, obtained by dividing all frequencies by the frequency value at the cross-over point, where $G' = G''$, and equally dividing all the

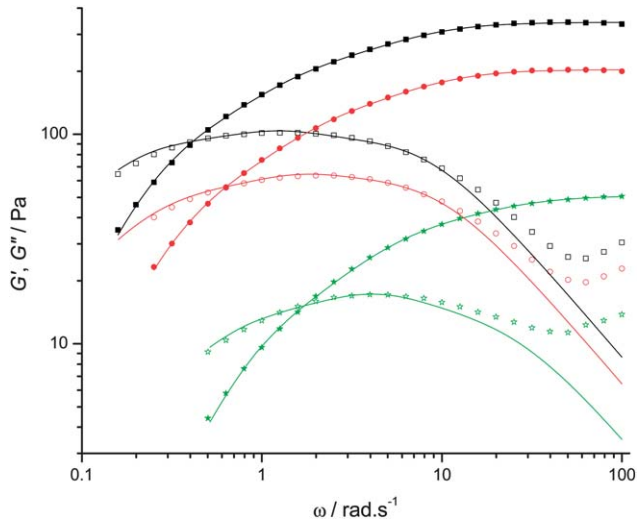

Fig. 1 Variation of the storage modulus G' (filled symbols) and loss modulus G'' (open symbols) as a function of the oscillatory shear frequency in solutions of 10% (■), 7.5% (●) and 5.0% (★) $ChEO_{10}$ with 5.0 wt% CMD. Solid lines are fits to the Maxwell model with 3 elements.

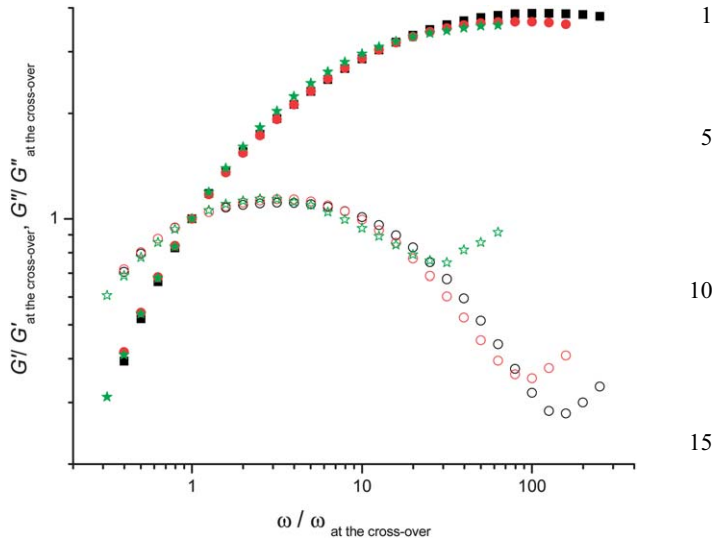

Fig. 2 A master curve of the three curves presented in Fig. 1: solutions of 10% (■), 7.5% (●) and 5.0% (★) $ChEO_{10}$ with 5.0 wt% CMD. The master curve was obtained by dividing all frequencies by the frequency value at the cross-over point ($G' = G''$), and equally dividing all the moduli by the respective moduli value at the cross-over point.

Table 1 Summary of the rheological parameters extracted from the frequency sweep measurements and viscosity curves of $ChEO_{10}$/CMD and $ChEO_{10}/C_{12}EO_3$/CMD solutions at 10%, 7.5% and 5.0% of $ChEO_{10}$ and fixed $ChEO_{10}/C_{12}EO_3$ ratio (5 : 1)

	$ChEO_{10}$/CMD			$ChEO_{10}/C_{12}EO_3$/CMD		
	5.0%	7.5%	10%	5.0%	7.5%	10%
G_1/Pa	14.7	59.3	109	20.2	29.4	54.3
G_2/Pa	23.7	75.6	123	31.4	34.0	60.9
G_3/Pa	12.5	68.6	110	28.8	56.9	62.8
G_4/Pa	—	—	—	23.7	55.3	66.1
G_5/Pa	—	—	—	14.6	24.5	138
G_0/Pa	50.9	204	342	119	200	382
G''_{dip}/Pa	11.3	19.6	25.5	19.4	43.9	—
τ_{r1}/s	1.2	2.9	4.0	52.2	72.0	34.0
τ_{r2}/s	0.24	0.61	0.81	6.70	5.55	4.70
τ_{r3}/s	0.05	0.14	0.16	0.92	0.730	0.69
τ_{r4}/s	—	—	—	0.15	0.120	0.097
τ_{r5}/s	—	—	—	0.02	0.013	0.008
τ_r/s	1.2	2.9	4.0	52.0	72.2	34.0
η_0/Pa s	29.9	367	688	—	—	—

moduli by the respective moduli value at the cross-over point. The curve obtained is shown in Fig. 2. All the frequency sweep curves overlap remarkably well, except at very high frequency, thus suggesting that the rheological changes observed are linked to a concentration effect rather than structural rearrangements.[63–65] As mentioned before, CMD aqueous solutions are turbid, suggesting the presence of aggregates of collapsed coils. CMD/$ChEO_{10}$ solutions instead are free of particles. This suggests that the micelles protect CMD's hydrophobic stickers from the solvent, allowing the coils to expand. Increasing the amount of surfactant correlates directly with an increase in active junction sites, by binding of the stickers from the polymer into the micelles, thus demonstrating a strong affinity of the polymer stickers for the micelles, as they associate with them rather than with themself.[64,66] This linear dependence of the rheological response with $ChEO_{10}$ concentration also supports the absence of entanglements; relaxation processes seem to be dominated by the association/dissociation of the hydrophobic stickers from the micellar aggregates. Note however that this concentration effect breaks up at 2.5% micelles, since the solutions remained liquid-like after adding the polymer, suggesting that this concentration of micelles is insufficient to provide connectivity. The master curve also highlights the departure from the model at high frequencies. For the systems studied here, the Maxwell behaviour holds as long as the relaxation processes are dominated by the dynamics of the junctions: as the frequency increases, this process becomes less important, while breathing or Rouse-like motion starts to dominate.[67] In the frequency sweeps, the transition is marked by a sudden increase of G'' in the high frequency range, deviating from the expected behaviour of the Maxwellian model. This departure taking place at the same frequency for all samples reflects the fact that while rheological parameters such as τ_r and G_0 depend on $ChEO_{10}$ concentration, the transition to breathing or Rouse-like relaxation processes depends on the nature of the supramolecular structures and not on their concentration.

The combination of $ChEO_{10}$ with $C_{12}EO_3$ leads to the growth of short $ChEO_{10}$ micelles into elongated wormlike micelles, as shown previously.[48,49] A more detailed structural characterisation of each type of micelles is presented in the next section (SANS measurements). For these WLM solutions, the ratio of surfactant/co-surfactant was kept constant at 5 : 1 (corresponding to the zero-shear viscosity peak) and $ChEO_{10}$ was varied from 2.5 to 10 wt% with 5.0 wt% of CMD, as for the shorter micelles.

The frequency sweeps for $ChEO_{10}/C_{12}EO_3$ alone are presented in Fig. 3. The systems behave as viscoelastic solids within the frequency range investigated with no visible cross-over point for G' and G''. Upon addition of the polymer, both moduli G' and G'' increase by one order of magnitude, however the solutions also become less solid-like with a larger G''/G' ratio throughout most of the frequency ranges studied. With the 2.5% $ChEO_{10}/C_{12}EO_3$

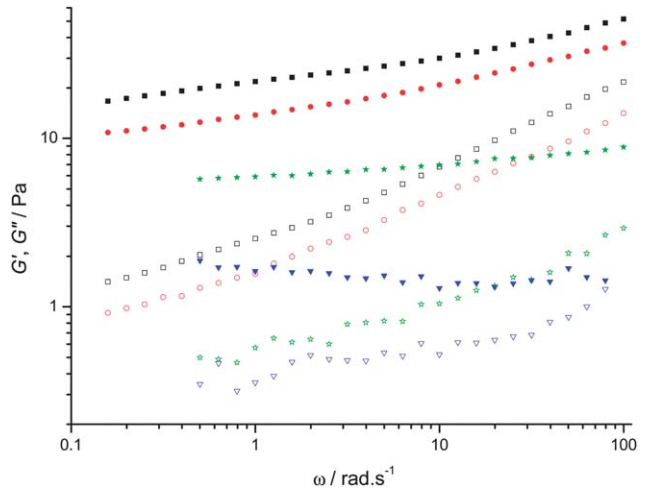

Fig. 3 Variation of the storage modulus G' (filled symbols) and loss modulus G'' (open symbols) as a function of oscillatory shear frequency in solutions of 10% $ChEO_{10}$/2.0% $C_{12}EO_3$ (■), 7.5% $ChEO_{10}$/1.5% $C_{12}EO_3$ (●), 5.0% $ChEO_{10}$/1.0% $C_{12}EO_3$ (★) and 2.5% $ChEO_{10}$/0.5% $C_{12}EO_3$ (▼).

system however, the addition of CMD induces a transition from a viscoelastic solid to a viscoelastic liquid, therefore showing the most significant contrast between $ChEO_{10}/C_{12}EO_3$ and $ChEO_{10}/C_{12}EO_3$/CMD systems. This drop in rheological response can be explained either by drastic structural changes, such as the breakup of micellar connectivity, or as dynamic changes giving rise to faster relaxation processes, such as branching.[68] As mentioned in the Introduction, both situations have been reported in WLM and polymer mixtures,[34,37,40,43] and it is difficult to distinguish one case from another based solely on the rheological data. However, given the striking change in the frequency sweep data (Fig. 4), together with the absence of a network formation at the same concentration of $ChEO_{10}$ short micelles (thus showing that this amount of short micelles is insufficient to provide junction points), we favour the hypothesis of a breakup of the WLM induced by CMD. SANS data presented in the next section give further support to this assumption. For all concentrations above 2.5%, the addition of CMD leads to a behaviour closer to the Maxwell model compared to the pure WLM, not too dissimilar to the one observed for the $ChEO_{10}$/CMD systems (Fig. 1), but with a larger spectrum of relaxation processes. Despite the obvious departure from the Maxwell behaviour, fits to a multi-elements Maxwell model were also performed here, purely as a mathematical tool, in order to extract and compare plateau modulus and relaxation time values and 'quantify' departure from the pure Maxwell model. Five elements were indeed needed to fit the frequency sweep curves (Table 1), which are presented in Fig. 4 as solid lines. The quality of the fits was much lower than for the $ChEO_{10}$/CMD system, even with the two additional elements. This clearly suggests a system with a wide range of relaxation times. This could possibly be explained by the presence of long, entangled micelles that are "sticked" by HMP, inducing several extra reptative relaxation modes of the entangled micelles by analogy with those predicted by the sticky reptation theory.[69,70] However another feature of this system that distinguishes it from the previous one (short micelles/CMD) is the presence of the co-surfactant, which may also influence the junctions lifetime. As for the $ChEO_{10}$/CMD system, we attempted to construct a master curve from the normalised frequency sweeps (Fig. 5). Due to the lack of a well-defined cross-over, the normalisation was based on an arbitrarily chosen frequency. The master curve for this system however does not show such a good superposition as the one observed for the $ChEO_{10}$/CMD systems (Fig. 2). This suggests that the changes seen in the rheological behaviour between 5.0% and 10% WLM

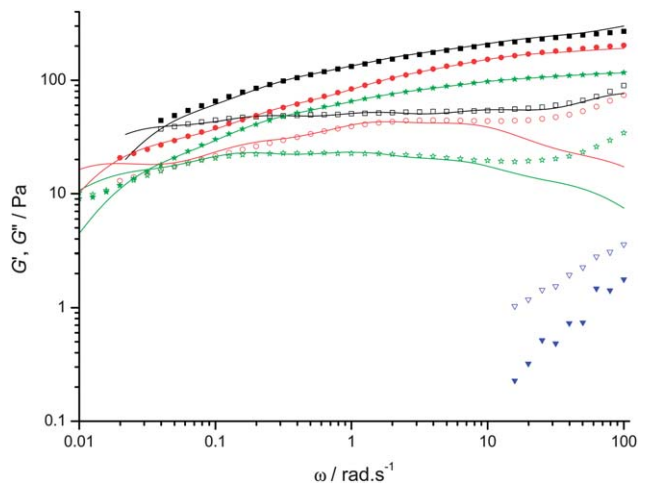

Fig. 4 Variation of the storage modulus G' (filled symbols) and loss modulus G'' (open symbols) as a function of oscillatory shear frequency in solutions of 5.0% CMD with 10% $ChEO_{10}$/2.0% $C_{12}EO_3$ (■), 7.5% $ChEO_{10}$/1.5% $C_{12}EO_3$ (●), 5.0% $ChEO_{10}$/1.0% $C_{12}EO_3$ (★) and 2.5% $ChEO_{10}$/0.5% $C_{12}EO_3$ (▼). Solid lines are fits to the Maxwell model with five elements.

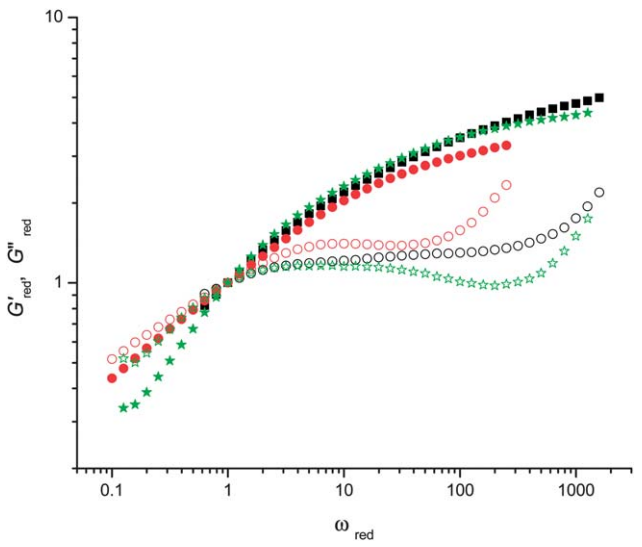

Fig. 5 A master curve of all three curves presented in Fig. 4 of solutions of CMD (5.0 wt%) with 10% $ChEO_{10}$/2.0% $C_{12}EO_3$ (■), 7.5% $ChEO_{10}$/1.5% $C_{12}EO_3$ (●) and 5.0% ChEO10/1.0% $C_{12}EO_3$ (★). The master curve was obtained by dividing all frequencies by an arbitrarily chosen frequency, and equally dividing all the moduli by the respective moduli value at the chosen frequency.

are not simply due to concentration effects. Given the complexity of the mixtures, it is difficult to pinpoint the structural differences which lead this result, however some hypotheses can be proposed. In the 2.5% WLM system, the change from a viscoelastic solid to a viscoelastic liquid suggested that CMD reduces end-cap energy, leading to micellar break up, therefore suppressing, or strongly reducing, their entanglement. Under this assumption then, it would be expected that at lower polymer/surfactant ratio (*i.e.* increasing $ChEO_{10}$ from 2.5% to 10%), micelles long enough to entangle may still be present. Therefore at increasing concentration, not only the number of polymer/micelles associative junctions is affected, but also the length of the micelles present, thus the balance between relaxation due to junction association and dissociation on one hand and micelles reptation is modified. If we suppose instead that micelles have been shortened down enough to suppress reptation, the possibility of a distribution of lengths, leading to slightly different junction dynamics (compared to the short micelles) could explain the non-linear change with concentration.

In the $ChEO_{10}$/CMD solutions, while all relaxation times τ_r followed a clear linear dependence with surfactant concentration, the same is not observed for the $ChEO_{10}/C_{12}EO_3$/CMD systems, where τ_r at the intermediate $ChEO_{10}$ concentration (7.5%) is higher than at the highest $ChEO_{10}$ concentration (10%), and τ_r at 10% of the surfactant is slightly lower than that at 5.0% (Table 1). The relaxation times are also much longer than for the equivalent short micelles system ($ChEO_{10}$/CMD), by an order of magnitude (Table 1). In comparison also, the breathing or Rouse modes are less clearly visible, although a slight upturn of G'' at high frequency would suggest that they are still present. Unlike the relaxation time, there is a clear trend in the plateau modulus G_0, which increases with concentration across the range studied.

Without yet making any assumption on the type of network formed, it is quite clear that junctions are created between the dextran cholesterol pendant groups and the hydrophobic tails of the surfactants, also cholesterol groups. The different viscoelastic behaviour between the two systems can be attributed to the different dynamics between short (rod-like) micelles and longer (broken wormlike) micelles: wormlike micelles have slow dynamics, implying longer hydrophobic junction lifetimes, thus longer relaxation times (Table 1). In addition, the density of connections is expected to be higher with the longer micellar aggregates than with the shorter near-spherical ones. The same long micelle could connect in several points along its length to either one or several polymer chains, thus giving rise to a combination of relaxation processes, both from the polymer and the longer micelles. These observations are reflected by the values of G_0, which relates to the junction density.[71] In both systems, G_0 increases with surfactant concentration and tends to reach similar values for both $ChEO_{10}/C_{12}EO_3$ and $ChEO_{10}/C_{12}EO_3$/CMD systems (G_0 values at 5.0% are quite different, while they are much closer at 7.5% and 10%, *cf.* Table 1). This reflects the different junction potential of both micellar aggregates: for the longer micelles, a larger number of connection sites is already established at the lowest concentration ($G_0 = 118$ Pa against 50.3 Pa for $ChEO_{10}$/CMD); as the concentration increases, the difference between G_0 for both systems is drastically reduced at the highest concentration ($G_0 = 382$ Pa against 341 Pa for $ChEO_{10}$/CMD).

The large deviation from the Maxwell behaviour for the $ChEO_{10}/C_{12}EO_3$/CMD when compared to the $ChEO_{10}$/CMD is not clear, but not surprising since the combination of long micelles with polymer is likely to give rise to a large spectrum of relaxation times. The nature of the distribution of the hydrophobic side chains along the polymeric backbone, probably irregular, may create local micro-domains with specific dynamics. For solutions of telechelic associative polymers and surfactants, a two-element Maxwell behaviour has been determined and was attributed to the existence of two relevant dynamics affecting the relaxation process: disruption of the hydrophobic junction and reptation of the micellar aggregates.[43] For telechelic associative polymers alone, one single relaxation time is expected, related to the dissociation of the hydrophobic junctions.[72] Curiously enough, both surfactant/polymer systems show a behaviour closer to the expected Maxwellian behaviour than the wormlike micelles alone, strongly suggesting that the polymer itself directs the overall system dynamics through the hydrophobic junction dissociation. Also, as mentioned above, in the $ChEO_{10}/C_{12}EO_3$ systems at 2.5% $ChEO_{10}$ concentration, CMD induces remarkable changes in the rheological behaviour, which we suggest is due to the loss of network connectivity caused by the breakup of the micellar aggregates.

Flow behaviour. The $ChEO_{10}$/CMD and $ChEO_{10}/C_{12}EO_3$/CMD systems studied in this work present a typical shear-thinning behaviour (Fig. 6). For the $ChEO_{10}$/CMD systems, a Newtonian plateau is observed in the lower shear rate range, up to a critical shear rate value where shear-thinning starts. The zero-shear viscosities (η_0) determined from the Newtonian plateau are very high (Table 1): at 10% $ChEO_{10}$/CMD, the viscosity is 688 Pa s, an increase of over 5 orders of magnitude compared to the pure micellar solutions (*ca.* 2 mPa s) at the same concentration, showing a remarkable synergistic effect. The viscosity increases linearly with concentration, from 5.0 to 10%.

The zero-shear viscosity (η_0) and the plateau modulus (G_0) are given by, respectively, $\eta_0 = \sum_k G_k \tau_k \leq G_0 \tau_r$[73] and $G_0 = \nu_{eff} RT$,[71] where R is the universal gas constant, T is the temperature and

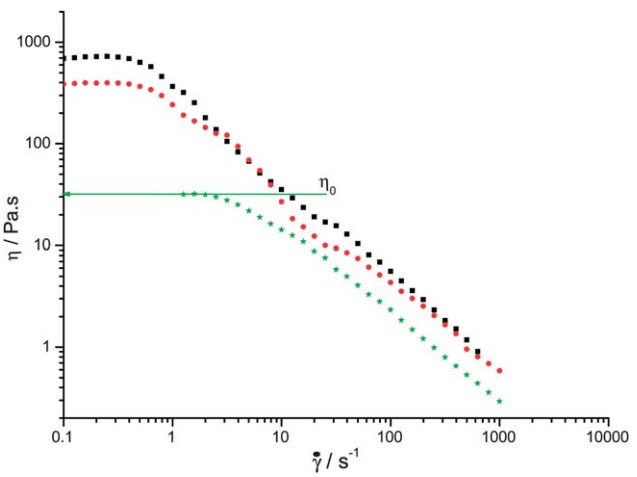

Fig. 6 Steady shear viscosity as a function of shear rate for a fixed concentration of CMD (5.0 wt%) and 10% (■), 7.5% (●) and 5.0% (★) $ChEO_{10}$.

ν_{eff} is the number of effective or active elastic chains, which is related to the junction density. Thus, the η_0 dependence on $ChEO_{10}$ concentration reflects the longer relaxation times and the higher junction density as the surfactant concentration increases. By using the relationship between G_0 and ν_{eff} it is possible to estimate a mesh size ξ, with $\xi \approx \sqrt[3]{1/\nu_{eff}}$. For the short micelles (with $G_0 = 50.9$, 206 and 342 Pa), we obtain $\xi \approx 432$ Å, 271 Å and 229 Å for 5.0, 7.5 and 10%, respectively. For the long micelles ($G_0 = 119$, 353 and 382 Pa), we obtain 326 Å, 227 Å and 201 Å, respectively, therefore (as expected) a decrease in mesh size with increasing micellar concentration and slightly denser networks with the long micelles, however more similar at the highest concentration studied (10%).

The flow curves for the $ChEO_{10}/C_{12}EO_3$/CMD system (Fig. 7) also show a typical shear-thinning behaviour. However, within the range of shear rates studied, no Newtonian plateau was observed. This may be a reflection of the larger increase of both relaxation time and entanglement density from $ChEO_{10}$/CMD to $ChEO_{10}/C_{12}EO_3$/CMD systems, increase larger enough to shift the Newtonian plateau to a lower shear region, outside the experimental window. The flow curves of the WLM without CMD are also quite similar (Fig. 7): the solutions shear-thin, without a measurable Newtonian plateau. The addition of polymer however increases the viscosity values by one order of magnitude, except at 2.5% of $ChEO_{10}/C_{12}EO_3$ where the presence of CMD causes a drastic viscosity reduction. This behaviour suggests that the CMD may disrupt the micellar aggregates, breaking them below entanglement level, and the amount of micelles and polymer in solution is below the percolation threshold[43] (as observed for 2.5% rod-like micelles). The small-angle neutron scattering results in the next section bring more support to this argument.

At low shear rates, the major contribution to viscosity comes from the junction points. As the shear rate increases, the macromolecules will orient under shear, possibly leading to a decrease of the lifetime of junction points.[74] At high enough shear rates, the dissociation of the junction points may lead to a breakup of the supramolecular structures. Thus at very high shear rates the hydrodynamic contribution of the oriented remaining aggregates is likely to be the major component, instead of the network junctions. The viscosity values at high shear for the $ChEO_{10}$/CMD and $ChEO_{10}/C_{12}EO_3$/CMD systems fall within a small region (1.9 to 5.6 Pa s at a shear rate of 100 s^{-1}), with the exception of the 10% wormlike micelle system ($ChEO_{10}/C_{12}EO_3$), which shows a value lower by an order of magnitude (~0.5 Pa s at 100 s^{-1}). This suggests that, once the bridging between the supramolecular aggregates is broken, the remaining elements are of similar size and shape for both systems within the concentration range studied, except perhaps for 10% $ChEO_{10}/C_{12}EO_3$, where we may have smaller aggregates. The shoulder seen in the $ChEO_{10}/C_{12}EO_3$/CMD at 10% of $ChEO_{10}$ flow curves can be attributed to the formation of shear-induced structures[75] or shear-banding,[76] as this flow instability at intermediate shear rates is a signature pattern of these types of phenomena and has been observed both in wormlike micelles[77,78] and associating polymer solutions.[79,80]

The rheological data show the remarkable effect of introducing CMD into the micellar solutions, both for the short and the long micelles. The strong synergy observed denotes very favourable associations between the micellar aggregates and the polymer, which is not surprising since their hydrophobic moieties are identical. Bridging between the polymer and the micelles is expected, which could be of two types, as described in the Introduction: in one scenario, the polymer creates bridges between large entangled micellar aggregates,[41] in another scenario, smaller spherical or rod-like micellar aggregates act as bridges between expanded polymer coils.[14] We could envisage the first type of network for the wormlike micelles ($ChEO_{10}/C_{12}EO_3$) and the second for the pure $ChEO_{10}$ shorter micelles. However the rheological data alone do not provide a clear picture of how the interactions take place. The SANS measurements presented in the following section provide a structural characterisation of the systems which enables us to clarify the nature of the associative networks formed.

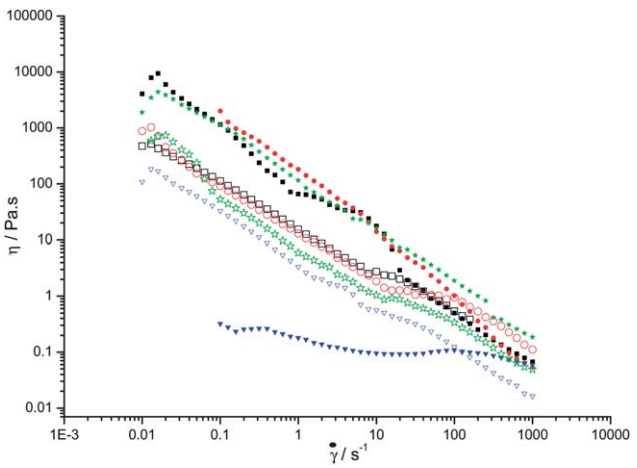

Fig. 7 Steady shear viscosity as a function of shear rate for a fixed concentration of CMD (5.0 wt%) and 10% $ChEO_{10}/2.0\%$ $C_{12}EO_3$ (■), 7.5% $ChEO_{10}/1.5\%$ $C_{12}EO_3$ (●), 5.0% $ChEO_{10}/1.0\%$ $C_{12}EO_3$ (★), 2.5% $ChEO_{10}/0.50\%$ $C_{12}EO_3$ (▼) and for the wormlike micelle solutions of 10% $ChEO_{10}/2.0\%$ $C_{12}EO_3$ (□), 7.5% $ChEO_{10}/1.5\%$ $C_{12}EO_3$ (○), 5.0% $ChEO_{10}/1.0\%$ $C_{12}EO_3$ (☆), 2.5% $ChEO_{10}/0.50\%$ $C_{12}EO_3$ (▽).

Structural study by small-angle neutron scattering measurements

Fig. 8 shows the SANS patterns from 1.0, 5.0 and 10% $ChEO_{10}$ solutions with and without the co-surfactant $C_{12}EO_3$. Structural information can be extracted from the dilute solutions (1.0%). At higher concentrations, the effect of the structure factor becomes clearly dominant as seen from the appearance of a marked interaction peak. The $ChEO_{10}$ micelles have been described as short rods or ellipsoids[48,49] and we were able to obtain reasonable fits with polydisperse spheres or ellipsoids (with an axial ratio of ~2), but the best fits were obtained with short rods of 42.5 ± 2.5 Å radius and 180 ± 20 Å (Fig. 8a). The length is in good agreement with the previously reported value of 17 nm.[48] The line of the fit does not follow the experimental plot closely in the high q region (Fig. 8a), which is in part due to instrumental smearing of the data as well as the possibility of an elliptical cross-section of the rods. These data are analysed in more detail in another publication,[51] however for our purpose here, assimilating the micelles to dense cylinders is a sufficient approximation, giving

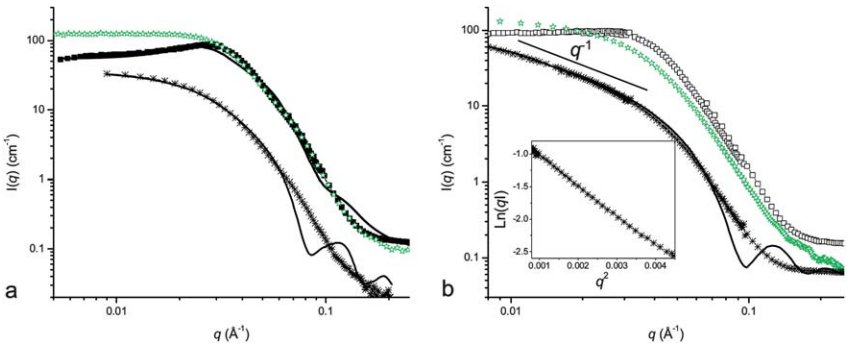

Fig. 8 (a) SANS experimental curves from $ChEO_{10}$ micellar solutions at 10% (■), 5.0% (★) and 1.0% (*) in D_2O. Solid lines are fits to the monodisperse rod model (for 1.0% ChEO10) and to the hard-sphere model for the 10% $ChEO_{10}$ solutions. (b) Scattering intensity $I(q)$ from SANS experiments on wormlike micellar solutions at 10% $ChEO_{10}$/2.0% $C_{12}EO_3$ (□), 5.0% $ChEO_{10}$/1.0% $C_{12}EO_3$ (☆) and 1.0% $ChEO_{10}$/0.20% $C_{12}EO_3$ (*) in D_2O. The solid line is a fit to a monodisperse rod model (1.0% $ChEO_{10}$/0.20% $C_{12}EO_3$). Inset: Kratky–Porod fit for 1.0% $ChEO_{10}$/0.20% $C_{12}EO_3$ scattering curve.

an aggregation number N_{agg} of *ca.* 800 by using the measured density of $ChEO_{10}$ of 1.065 g cm^{-3}. Addition of $C_{12}EO_3$ promotes the one-dimensional growth of $ChEO_{10}$ micelles by intercalating between the large polyoxyethylene headgroups and thus decreasing the headgroup surface area. This leads to a clear change of the scattering pattern in the low q region, where the intensity follows a q^{-1} power law (1% $ChEO_{10}$/0.2% $C_{12}EO_3$), which is a clear signature of rods (Fig. 8b). The scattering at high q remains unchanged, showing that the cross-section is not affected by the growth. A Kratky–Porod representation of the data in ln (qI) *vs.* q^2 gives a linear plot over a wide q-range (Fig. 8b, inset), confirming the presence of elongated cylindrical structures, from which the radius of the cross-section and the mass per unit length can be extracted and were $R = 41 \pm 2$ Å and $M_L = 3.0 \pm 0.5$ kg mol^{-1} $Å^{-1}$. By considering a volume of cylinder of length 1 Å and of the density of $ChEO_{10}$, we obtain a reasonably close value of 4 kg mol^{-1} $Å^{-1}$. Fitting the data to a monodisperse rod model confirms a cross-section of $R = 40 \pm 2.5$ Å and contour length $L \approx 400$ Å (the fit however is not sensitive to the value of L because it is outside the SANS measurement window, as seen by the absence of a plateau at low q). At a higher WLM concentration of 5.0% $ChEO_{10}$/1.0% $C_{12}EO_3$ (ratio unchanged), the q^{-1} behaviour is still detectable but interactions start to modify the pattern. In comparison, the scattering from the 'short' micelles at the same concentration (Fig. 8a) shows a flat plateau, indicative of a finite length. At higher concentrations (10%), the scattering in both systems is dominated by strong interactions. A reasonable fit is obtained for the short $ChEO_{10}$ micelles with a model of spheres of 42.5 ± 2.5 Å interacting through a hard-sphere potential (Fig. 8a). Given that the rods are short (the length is about twice the cross-section diameter) and that interactions dominate the scattering pattern, it is not surprising that a simple hard-sphere model is sufficient to describe the data. At the same concentration in the mixed surfactants system (Fig. 8b) very long wormlike micelles are observed, with lengths well above 1 μm, as seen from the cryo-TEM image of 10% $ChEO_{10}$ with 2.0% $C_{12}EO_3$ (Fig. 9).

The addition of 5.0% modified dextran to the solutions of both short ($ChEO_{10}$) and long ($ChEO_{10}/C_{12}EO_3$) micelles is expected to give rise to a connected network, through cholesterol–cholesterol hydrophobic interactions between the dextran stickers and the micelles interiors. Given the different rheological

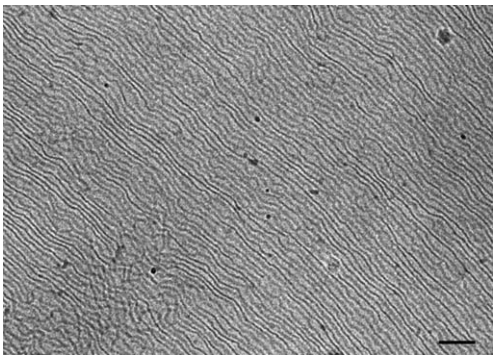

Fig. 9 Cryo-TEM image of wormlike micelles in 10% $ChEO_{10}$ and 2.0% $C_{12}EO_3$ aqueous solution.

behaviour obtained for these two systems (short and long micelles with CMD), quite different SANS patterns were expected. Quite surprisingly instead, the scattering curves from all samples at each concentration are seen to superimpose almost perfectly (Fig. 10) at each polymer/micelles ratio, suggesting a similar type of organisation. To show this more clearly, the scattering from 7.5% solutions of both short and long rods with CMD is presented in the inset of Fig. 10. The scattering of a filtered solution of polymer alone is also reproduced as a reference; it clearly shows no similarity with the patterns obtained from the mixed systems. The scattering of the polymer/micelles networks is dominated by strong interactions, with a clear structural peak. The peak position only shifts slightly with concentration, and is reminiscent of the peak observed in pure $ChEO_{10}$ micellar solutions at 10%, which is reproduced in Fig. 10 for comparison purposes; however, the interactions are stronger, as seen from the stronger depression of the intensity at low q. The data can be approximated to a system of interacting hard spheres (Fig. 10), with a radius of 42.5 ± 2.5 Å and polydispersity $\sigma/\bar{R} = 0.2$, accounting for the possibility of more elongated structures (short rods) rather than spheres. Closer examination of the data shows that the structural peak shifts very slightly to lower q from 10% to 7.5% micelles, and in a more pronounced way from 7.5% to 5.0%, with a slight decrease of the intensity in the latter case. The narrow shape of the peaks suggests assimilating the scattering maxima q^* to a Bragg peak, with $d = 2\pi/q^*$, where d is an

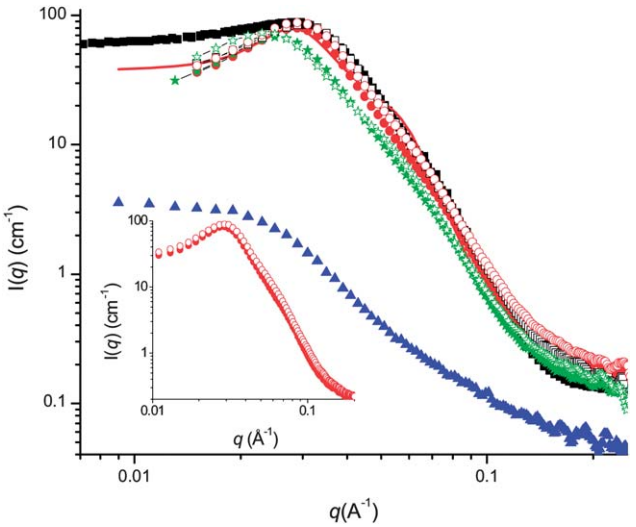

Fig. 10 SANS experimental curves from 5.0 wt% CMD (▲), with short rod-like micelles (7.5% $ChEO_{10}$ (●), 5.0% $ChEO_{10}$ (★)) and wormlike micelle solutions ($ChEO_{10}/C_{12}EO_3$ at 10% $ChEO_{10}$ (□), 7.5% $ChEO_{10}$/1.5% (○) and 5.0% $ChEO_{10}$/1.0% $C_{12}EO_3$ (☆)) in D_2O. For comparison 10% $ChEO_{10}$ micelles without CMD (■) are also shown. The solid line is a fit to the hard-sphere model. Inset: scattering curves of 7.5% $ChEO_{10}$ (●) and 7.5% $ChEO_{10}$/1.5% $C_{12}EO_3$ (○) with 5.0 wt% CMD.

estimate of the average size of the scattering density fluctuations, or network mesh size. A similar scattering pattern and interpretation have been reported for lysozyme gels.[81] With this approach, we obtain mesh sizes of 273 Å, 233 Å and 217 Å for 5.0, 7.5 and 10% micelles, respectively (corresponding to q = 0.023, 0.027 and 0.029 $Å^{-1}$), independently of the nature of the micelles. Although a very rough approximation, these mesh sizes are comparable to the ones obtained from the plateau modulus G_0 in the previous section and very close to the values calculated assuming that the micelles are simply arranged in a cubic lattice with $N_{agg} \approx 800$ (*cf.* above): 278 Å, 243 Å and 221 Å for 5.0, 7.5 and 10% micelles, respectively. It is of course expected that given the polydispersity of the micelles and polymer, heterogeneity of the cholesterol stickers distribution along the chains, the network is not perfectly uniform and regular as the value of a 'mesh size' would suggest. However, the picture emerging from the SANS data is overall the one of a network dominated by the scattering from a relatively ordered distribution of junctions of finite size, roughly the size of the individual $ChEO_{10}$ micelles. The most striking result is that the structure of the network seems to be identical in the case of the short (rods) and the long (wormlike) micelles. On the basis of this evidence, we tentatively propose that the network is dominated by the polymer chains which act as bridges between the micelles, as represented in Scheme 1, rather than the polymer cross-linking the wormlike micelles, as was found in other studies.[41,45,69] Neutrons in this case are sensitive to the higher density regions formed by the junction zones (which we suggest are short rods) rather than the extended polymer chains, which scatter less. In this scenario, the association between CMD and the mixed-surfactant wormlike micelles leads to the breakup of the long (wormlike) micelles in order to shield more efficiently the pendent cholesterol groups from the solvent. In the case of the WLM, favourable interactions between the

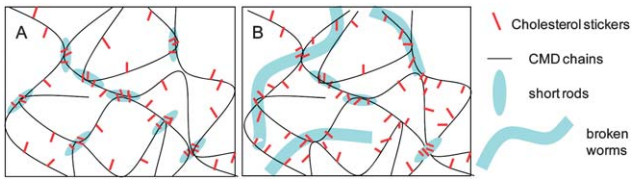

Scheme 1 Schematic representation of the proposed networks formed by adding the modified dextran to solutions of (A) short $ChEO_{10}$ rods and (B) $ChEO_{10}/C_{12}EO_3$ wormlike micelles. In both cases, the elasticity of the network arises from polymer chains connected by micellar junctions through cholesterol–cholesterol interactions. In the case of $ChEO_{10}/C_{12}EO_3$ mixtures (B), the worms break down by interacting with the polymer, but it is expected that a distribution of lengths is still present, thus explaining the large spectrum of relaxation times in the rheological behaviour.

cholesterol groups from the $ChEO_{10}$ surfactant and the polymer could lead to the extraction of the co-surfactant ($C_{12}EO_3$) from the micelles, therefore favouring the rod-to-sphere transition. The hypothesis of a breakup of the wormlike micelles by CMD is strongly reinforced by the observation that at 2.5% WLMs, the solutions lost their solid-like behaviour when adding the polymer. Since, in the equivalent 2.5% $ChEO_{10}$ system, the samples remained liquid-like, this suggests that short rod-like micelles are present in both, and an insufficient number of them to provide a network connecting the CMD chains through their stickers. By assimilating the micelles to cylinders of 42.5 Å radius and 180 Å length, we would have at 2.5% concentration 2.3×10^{16} micelles per cm^3 and 1.8×10^{18} cholesterol stickers. At 5.0% $ChEO_{10}$ and 4.6×10^{16} micelles per cm^3, we have a sufficient number of junctions to form a network and at 10% (9.3×10^{16} micelles per cm^3) still a large excess of CMD hydrophobes (1 micelle per ~20 stickers), suggesting that networks of higher strength could still be obtained at higher micellar concentrations.

Given however the different rheological response of the two systems, it is expected that some distribution of lengths still exists in the $ChEO_{10}/C_{12}EO_3$ micelles (Scheme 1B), accounting for the larger spectrum of relaxation times observed from the frequency sweep data (Fig. 4 and Table 1); in addition the presence of the co-surfactant may also influence the junctions lifetime. It is unlikely that slightly longer rods would be detected by SANS, since the scattering is dominated by strong interactions arising from the junction points; however the presence of long wormlike micelles would be expected to change the patterns to some extent. Therefore, we cannot exclude the presence of longer micelles in the $ChEO_{10}/C_{12}EO_3$/CMD systems, however the combination of the SANS data with the rheology experiments, which suggested a micellar breakup at 2.5% WLM (Fig. 4), as well as the occurrence of structural rearrangements with increasing $ChEO_{10}/C_{12}EO_3$ concentration (Fig. 5), all concur to give the picture that we propose in Scheme 1. We note that small structural differences that are undetected by SANS (or cryo-TEM) can lead to a very different rheological behaviour, as we have previously reported in a system of wormlike micelles with hydrophobic solutes.[40] Very subtle changes in self-assembly structures can lead to large changes in the rheological response by adding or removing relaxation processes. This is a point that we feel would deserve more discussion in the literature. This highlights again the necessity of using both techniques in combination to achieve

a better understanding of the systems: probing bulk *and* dynamic aspects (rheology) as well nanoscopic organization (scattering).

Overall, the dynamics of the system are therefore dominated by the association/dissociation processes of the polymer/micelles junctions. By anchoring into the micellar cores, and possibly partially wrapping around the micelles, the polymer creates strong repulsions between the micelles, evidenced by the structural peak in the scattering pattern. The synergy between polymer and micelles is such that micelles are able to uncoil the polymer chains, which were collapsed and aggregated in solution, and act as connecting points between the long polymeric chains, building-up a strong mixed network.

Conclusion

In this work we have reported that the addition of a cholesterol-modified dextran (CMD) to short and long micelles of polyoxyethylene cholesteryl ether ($ChEO_{10}$) leads to a strong synergistic behaviour, inducing the formation of a strong network. $ChEO_{10}$ forms short (rod-like) micelles in aqueous solutions, which exhibit a weak Newtonian behaviour in the concentration range studied. The addition of 5.0 wt% CMD to these solutions (up to 10 wt% micelles) induces a strong viscoelastic behaviour, with a significant increase of the zero-shear viscosity, from *ca.* 2 mPa s to 688 Pa s. The frequency sweep curves follow a near-Maxwellian behaviour (with 3 elements), suggesting the formation of a solid-like network of mixed polymer and micelles. At the lowest concentration studied of 2.5 wt% micelles however, the behaviour remains liquid-like, suggesting that the number of cross-links is insufficient to form a network. A remarkable superposition of the frequency-sweep curves (when normalised by the G' and G'' cross-over points) suggests that changes in rheology with increasing micelle/polymer ratio can be attributed solely to concentration effects, namely, the addition of connection points.

The addition of small amounts of the lipophilic co-surfactant triethylene glycol monododecyl ether ($C_{12}EO_3$) to $ChEO_{10}$ solutions (in a 1 : 5 ratio) leads to the uni-dimensional growth of the short rod-like micelles into wormlike micelles (WLMs), which show strong viscoelastic properties. The addition of 5.0 wt% CMD to the WLM solutions leads to a strong associative behaviour, characterised by the increase of G' and G'' by one order of magnitude in addition to higher low-shear viscosity, reaching *ca.* 10 000 Pa s. However, CMD/WLM solutions exhibit a more liquid-like behaviour than the pure WLMs, as suggested by the decrease of the G''/G' ratio. Interestingly at the lowest WLM concentration studied (2.5 wt%), the samples become more liquid-like when adding the polymer, suggesting a breakup of the long micellar aggregates and an insufficient number of crosslinks to form a network, as was observed at the same concentration with the short micelles. The frequency sweep data depart from the Maxwellian behaviour, pointing to a wide spectrum of relaxation times. The frequency-sweep curves do not superimpose as well as for the previous system, suggesting that structural changes are occurring with increasing micelle/polymer ratio, which are quite likely linked to the breakup of the worms.

Overall, the rheological data show the remarkable effect of introducing CMD into the micellar solutions, both for the short and the long micelles, due to cholesterol–cholesterol associations between the micellar aggregates and the polymer.

Small-angle neutron scattering (SANS) measurements reveal a very similar network for both systems: one dominated by the scattering of micellar junctions which act as cross-links between the polymeric chains, through cholesterol–cholesterol hydrophobic interactions. The combination of rheology results with SANS therefore concur to suggest that the WLMs are broken-up into shorter rods by the polymer, therefore giving a rheological response not too dissimilar from the one in the network of shorter micelles, with however a wider spectrum of relaxation processes attributed to a distribution of lengths and possibly the presence of the co-surfactant.

Acknowledgements

HA and CAD acknowledge ISIS and HZB for the provision of beam time and the European Commission for financial support under the 6th Framework Programme through the Key Action: Strengthening the European Research Infrastructures (contract no.: RII3-CT-2003-505925 (NMI 3)). Travel funds (HA, CN, JLS and CAD) were obtained from the British Council under the Alliance Franco-British Partnership Programme. HA acknowledges King's College London for the award of a PhD studentship. We are very grateful to Göran Karlsson for the cryo-TEM measurements of the wormlike micelles and to Simon Ross-Murphy for very helpful discussions.

References

1 L. J. Magid, *J. Phys. Chem. B*, 1998, **102**, 4064–4074.
2 A. K. Sood, R. Bandyopadhyay and G. Basappa, *Pramana—Journal of Physics*, 1999, **53**, 223–235.
3 C. A. Dreiss, *Soft Matter*, 2007, **3**, 956–970.
4 S. J. Candau, G. Waton, F. Merikhi and R. Zana, *Macromolecular Liquids*, 1990, **177**, 143–146.
5 M. E. Cates, *J. Phys. Chem.*, 1990, **94**, 371–375.
6 F. K. Rubin and D. V. Blarcom, *Viscose Compositions Containing Amido Betaines and Salts*, 1983.
7 K. Dismuke. M. Samuel, R. J. Card, J. E. Brown and K. W. England, *Methods of Fracturing Subterranean Formations*, 2001.
8 G. J. Tustin and T. G. Jones, *Gelling Composition for Wellbore Service Fluids*, 2001.
9 L. C. Chou, R. N. Christenen and J. L. Zakin, *The Influence of Chemical Composition of Quaternary Ammonium Salt Cationic Surfactants for District Heating and Cooling*, 1989, pp. 141–149.
10 I. Harwigsson and M. Hellsten, *J. Am. Oil Chem. Soc.*, 1996, **73**, 921.
11 W. Smith, *Viscoelastic Cleaning Compositions with Long Relaxation Times*, 1995.
12 D. Balzer, *Aqueous Viscoelastic Surfactant Solutions for Hair and Skin Cleaning*, 1999.
13 S. Talwar, J. Harding, K. R. Oleson and S. A. Khan, *Langmuir*, 2009, **25**, 794–802.
14 S. Talwar, L. Scanu, S. R. Raghavan and S. A. Khan, *Langmuir*, 2008, **24**, 7797–7802.
15 S. Talwar, L. F. Scanu and S. A. Khan, *J. Rheol.*, 2006, **50**, 831–847.
16 J. H. Lee, J. P. Gustin, T. H. Chen, G. F. Payne and S. R. Raghavan, *Langmuir*, 2005, **21**, 26–33.
17 E. Rotureau, E. Dellacherie and A. Durand, *Eur. Polym. J.*, 2006, **42**, 1086–1092.
18 Y. Y. Chieng and S. B. Chen, *J. Colloid Interface Sci.*, 2010, **349**, 236–245.
19 P. Chiewpattanakul, R. Covis, R. Vanderesse, B. Thanomsub, E. Marie and A. Durand, *Colloid Polym. Sci.*, 2010, **288**, 959–967.
20 C. Nouvel, C. Frochot, V. Sadtler, P. Dubois, E. Dellacherie and J. L. Six, *Macromolecules*, 2004, **37**, 4981–4988.

21 L. Dupayage, M. Save, E. Dellacherie, C. Nouvel and J. L. Six, *J. Polym. Sci., Part A: Polym. Chem.*, 2008, **46**, 7606–7620.
22 *Water-Soluble Polymers for Petroleum Recovery*, ed. D. G. A. Stahl and N. Schultz, Plenum Press, New York, 1986.
23 J. E. Glass, Polymers in Aqueous Media: Performance Through Association, *Advances in Chemistry Series 223*, American Society, Washington, 1989.
24 O. Quadrat and J. Snuparek, *Prog. Org. Coat.*, 1990, **18**, 207–228.
25 R. D. Jenkins, C. A. Silebi and M. S. Elaasser, *Polymers as Rheology Modifiers*, American Chemical Society, Washington, DC, 1991.
26 Y. L. Chiu, S. C. Chen, C. J. Su, C. W. Hsiao, Y. M. Chen, H. L. Chen and H. W. Sung, *Biomaterials*, 2009, **30**, 4877–4888.
27 N. Dew, K. Edwards and K. Edsman, *Colloids Surf., B*, 2009, **70**, 187–197.
28 C. Nouvel, J. Raynaud, E. Marie, E. Dellacherie, J. L. Six and A. Durand, *J. Colloid Interface Sci.*, 2009, **330**, 337–343.
29 J. A. Shashkina, O. E. Philippova, Y. D. Zaroslov, A. R. Khokhlov, T. A. Pryakhina and I. V. Blagodatskikh, *Langmuir*, 2005, **21**, 1524–1530.
30 I. Couillet, T. Hughes, G. Maitland and F. Candau, *Macromolecules*, 2005, **38**, 5271–5282.
31 I. Iliopoulos, T. K. Wang and R. Audebert, *Langmuir*, 1991, **7**, 617–619.
32 O. E. Philippova, D. Hourdet, R. Audebert and A. R. Khokhlov, *Macromolecules*, 1996, **29**, 2822–2830.
33 O. E. Philippova and S. G. Starodoubtzev, *J. Polym. Sci., Part B: Polym. Phys.*, 1993, **31**, 1471–1476.
34 Z. C. Lin and C. D. Eads, *Langmuir*, 1997, **13**, 2647–2654.
35 S. Panmai, R. K. Prud'homme, D. G. Peiffer, S. Jockusch and N. J. Turro, *Langmuir*, 2002, **18**, 3860–3864.
36 T. Noda, A. Hashidzume and Y. Morishima, *Langmuir*, 2000, **16**, 5324–5332.
37 C. Flood, C. A. Dreiss, V. Croce, T. Cosgrove and G. Karlsson, *Langmuir*, 2005, **21**, 7646–7652.
38 G. Massiera, L. Ramos and C. Ligoure, *Langmuir*, 2002, **18**, 5687–5694.
39 V. S. Molchanov, O. E. Philippova, A. R. Khokhlov, Y. A. Kovalev and A. I. Kuklin, *Langmuir*, 2007, **23**, 105–111.
40 K. R. Francisco, M. A. da Silva, E. Sabadini, G. Karlsson and C. A. Dreiss, *J. Colloid Interface Sci.*, 2010, **345**, 351–359.
41 T. P. Lodge, R. Taribagil, T. Yoshida and M. A. Hillmyer, *Macromolecules*, 2007, **40**, 4728–4731.
42 T. Yoshida, R. Taribagil, M. A. Hillmyer and T. P. Lodge, *Macromolecules*, 2007, **40**, 1615–1623.
43 T. Tixier, H. Tabuteau, A. Carriere, L. Ramos and C. Ligoure, *Soft Matter*, 2010, **6**, 2699–2707.
44 J. C. Brackman and J. Engberts, *J. Am. Chem. Soc.*, 1990, **112**, 872–873.
45 L. Ramos and C. Ligoure, *Macromolecules*, 2007, **40**, 1248–1251.
46 B. J. K. Holmberg, B. Kronberg and B. Lindman, *Surfactants and Polymers in Aqueous Solutions*, Wiley, New York, 2002.
47 T. Sato, M. K. Hossain, D. P. Acharya, O. Glatter, A. Chiba and H. Kunieda, *J. Phys. Chem. B*, 2004, **108**, 12927–12939.
48 C. Moitzi, N. Freiberger and O. Glatter, *J. Phys. Chem. B*, 2005, **109**, 16161–16168.
49 D. P. Acharya and H. Kunieda, *J. Phys. Chem. B*, 2003, **107**, 10168–10175.
50 T. Ahmed and K. Aramaki, *J. Colloid Interface Sci.*, 2008, **327**, 180–185.
51 H. Afifi, G. Karlsson, R. K. Heenan and C. A. Dreiss, *Langmuir*, 2011, submitted.
52 K. Akiyoshi, S. Deguchi, N. Moriguchi, S. Yamaguchi and J. Sunamoto, *Macromolecules*, 1993, **26**, 3062–3068.
53 R. K. Heenan, S. M. King, R. Osborn and H. B. Stanley, *RAL Intl. Rep.*, 1989, 89–128.
54 S. M. King, *Modern Techniques for Polymer Characterisation*, John Wiley and Sons, Ltd, 1999.
55 O. Kratky and G. Porod, *Recl. Trav. Chim. Pays-Bas*, 1949, **68**, 1106.
56 R. Heenan, in Rutherford-appleton laboratory, Chilton, Didcot, UK, 2003.
57 T. Shikata, M. Shiokawa and S. Imai, *J. Colloid Interface Sci.*, 2003, **259**, 367–373.
58 J. P. Zhou, Y. G. Shangguan, Q. Wu and Q. Zheng, *Polym. Int.*, 2009, **58**, 1275–1282.
59 C. Goncalves, J. A. Martins and F. M. Gama, *Biomacromolecules*, 2007, **8**, 392–398.
60 T. Annable, R. Buscall, R. Ettelaie and D. Whittlestone, *J. Rheol.*, 1993, **37**, 695–726.
61 C. Rufier, A. Collet, M. Viguier, J. Oberdisse and S. Mora, *Macromolecules*, 2008, **41**, 5854–5862.
62 V. Tirtaatmadja, K. C. Tam and R. D. Jenkins, *AIChE J.*, 1998, **44**, 2756–2765.
63 J. S. Bernardes, M. A. da Silva, L. Piculell and W. Loh, *Soft Matter*, 2010, **6**, 144–153.
64 L. Piculell, M. Egermayer and J. Sjostrom, *Langmuir*, 2003, **19**, 3643–3649.
65 A. Y. Malkin, *Rheology Fundamentals*, ChemTec Publishing, Toronto, 1994.
66 C. Rufier, A. Collet, M. Viguier, J. Oberdisse and S. Mora, *Macromolecules*, 2009, **42**, 5226–5235.
67 R. Granek, *Langmuir*, 1994, **10**, 1627–1629.
68 R. Granek and M. E. Cates, *J. Chem. Phys.*, 1992, **96**, 4758–4767.
69 K. Nakaya-Yaegashi, L. Ramos, H. Tabuteau and C. Ligoure, *J. Rheol.*, 2008, **52**, 359–377.
70 L. Leibler, M. Rubinstein and R. H. Colby, *Macromolecules*, 1991, **24**, 4701–4707.
71 M. S. Green and A. V. Tobolsky, *J. Chem. Phys.*, 1946, **14**, 80–92.
72 L. Pellens, R. G. Corrales and J. Mewis, *J. Rheol.*, 2004, **48**, 379–393.
73 H. Rehage, *J. Phys. Chem.*, 1988, **92**, 4712.
74 F. Tanaka and S. F. Edwards, *Macromolecules*, 1992, **25**, 1516–1523.
75 Y. T. Hu, S. Q. Wang and A. M. Jamieson, *J. Rheol.*, 1993, **37**, 531–546.
76 B. Yesilata, C. Clasen and G. H. McKinley, *J. Non-Newtonian Fluid Mech.*, 2006, **133**, 73–90.
77 F. Bautista, J. F. A. Soltero, J. H. Perez-Lopez, J. E. Puig and O. Manero, *J. Non-Newtonian Fluid Mech.*, 2000, **94**, 57–66.
78 E. Miller and P. Rothstein, *J. Non-Newtonian Fluid Mech.*, 2007, **143**, 22–37.
79 H. Tabuteau, L. Ramos, K. Nakaya-Yaegashi, M. Ima and C. Ligoure, *Langmuir*, 2009, **25**, 2467–2472.
80 J. Sprakel, E. Spruijt, M. A. Choen Stuart, N. A. M. Besseling, M. P. Lettinga and J. van der Gucht, *Soft Matter*, 2008, **4**, 1606–1705.
81 H. Yan, H. Frielinghaus, A. Nykanen, J. Ruokolainen, A. Saiani and A. F. Miller, *Soft Matter*, 2008, **4**, 1313–1325.

Authors Queries

Journal: **SM**

Paper: **c1sm05416c**

Title: **Associative networks of cholesterol-modified dextran with short and long micelles**

Editor's queries are marked like this... **1**, and for your convenience line numbers are inserted like this... 5

Query Reference	Query	Remarks
1	For your information: You can cite this article before you receive notification of the page numbers by using the following format: (authors), Soft Matter, (year), DOI: 10.1039/c1sm05416c.	
2	Do you wish to add an e-mail address for the corresponding author?	
3	Please indicate the boiling range of the petroleum ether used here (*e.g.* 40–60 °C).	
4	The values for 'G_0' (118 Pa, 50.3 Pa, and 341 Pa) quoted in the sentence beginning 'This reflects the different junction…' do not appear to match those given in Table 1, please check this carefully and indicate any changes that are required.	
5	Ref. 4: please give the name of this journal in full, including any other names by which this journal may be known, so that its CASSI abbreviation can be checked for indexing purposes.	
6	Ref. 51: Can this reference be updated yet? Please supply details to allow readers to access the reference (for references where page numbers are not yet known, please supply the DOI).	
7	Ref. 56: Please provide the following details: book title.	